Electrostatic screening near semiconductor surfaces

Maja Krčmar, Wayne M. Saslow, and Michael B. Weimer
Department of Physics, Texas A&M University, College Station, Texas 77843-4242
(Received 5 August 1999; revised manuscript received 9 December 1999)

We have developed a semimicroscopic theory for the electrostatic potential due to an isolated charge near a semiconductor surface whose surface states do not contribute free carriers. It employs the linearized version of the Debye-Hückel (or, equivalently, the Thomas-Fermi) approximation. This includes the screening effects both of the plasma of free carriers due to bulk donors or acceptors, and of the bound polarizable charge associated with the bulk dielectric, but does not include free charge from intrinsic or extrinsic surface states. Results are obtained for a source charge above the semiconductor, within the semiconductor, and on the semiconductor surface, but we emphasize the last case. Although there is a dipole moment associated with source charge on the surface, the surface potential at long distances is quadrupolar; at intermediate distances greater than a characteristic atomic dimension it is a screened exponential, with screening length equal to the bulk value. The case of intermediate distance provides a rigorous basis for the exponentially screened surface potential commonly employed to analyze scanning tunneling microscopy images of the depletion or accumulation regions surrounding isolated charges on III-V(110) cleavage surfaces. Certain of these results also apply to colloids.

I. INTRODUCTION

Electrostatic screening near semiconductor surfaces is a fundamental problem with many ramifications. In the present work we develop a comprehensive picture of the screening of point charges at ideal III-V(110) cleavage surfaces for which the intrinsic surface states lie outside the band gap.[1] These states thus are either completely filled or completely empty, and therefore are insulating. The theory includes the screening effects of the plasma of free carriers due to donors or acceptors in the bulk, and of the bound charge associated with the dielectric. However, it does not account for the free surface charge contributed by a partially filled band of intrinsic or extrinsic surface states. Because of the similarities between such ideal semiconductors and colloids, certain of our results for semiconductors also apply to colloids. These are both examples of coupled plasma-dielectric problems, where there is a large dielectric constant due to polarizable bound charge (the atoms for semiconductors, water molecules for colloids) and a significant density of free bulk carriers (electrons and holes for semiconductors, ions for colloids).

Our analysis is based on the linearized version of Debye-Hückel (or, equivalently, Thomas-Fermi) theory; restriction to the linear regime means that the theory applies when variations in the electrical potential energy are smaller than k_BT. This picture is semimicroscopic, rather than microscopic, and makes use of experimental quantities, such as the density of the free carriers and the dielectric constant of the bound electrons; it therefore applies only on length scales larger than a characteristic atomic length a. An entirely microscopic theory of electrostatic screening in semiconductors would differ from ours only at short distances. It would give a specific value for the dielectric constant appropriate to screening by bound charge at the surface, and it would give the specific value of the valence associated with any surface defects. In our work, we take the surface dielectric constant to equal the bulk dielectric constant (although this could be modified, if necessary), and we take the valence of the perturbing surface charge to be a fitting parameter determined from experiment.

We consider the screening of an isolated source charge q located above the semiconductor, within the semiconductor bulk, or on the semiconductor surface; it is the last case, in particular, that calls attention to the need for a comprehensive theory. It is known empirically that the scanning tunnel microscopy (STM) contours surrounding an individual III-V(110) surface charge exhibit a spatially varying envelope due to majority carrier depletion (or accumulation, depending on the sign of the perturbing charge) that decays with distance from the source. This decay is consistent, in the case of dilute surface concentrations, with a screened Coulomb potential whose screening length R_b is governed by the bulk carrier density.[2] However, there is no rigorous *a priori* justification why this functional dependence should hold at the surface. In a more recent STM study involving much higher surface defect concentrations, the interaction energy between two surface charges as a function of separation, $U(\rho)$, was deduced from the spatial distribution of anion vacancies at the (110) surface of InP.[3] The authors of this study assumed $U(\rho)$ to be the product of the charge q of one vacancy and the surface potential $\phi_s(\rho)$ due to the other, with $\phi_s(\rho)$ a screened Coulomb interaction parametrized by

$$\phi_s(\rho)=\frac{q}{4\pi\varepsilon_0\varepsilon_{eff}\rho}\exp(-\rho/R_s). \tag{1}$$

Here ε_0 is the dielectric constant of free space, ε_{eff} is an effective dielectric constant given by $\varepsilon_{eff}=(\varepsilon+1)/2$, and R_s an empirically determined surface screening length. Equation (1) yielded a satisfactory fit to the data with $|q|=1e$ and R_s about a factor of 3 smaller than R_b. Again, as correctly noted in Ref. 3, there is no *a priori* theoretical basis for the assumed form (1).

The structure of this paper is as follows. Section II gives an overview of screening in an infinite medium, distinguishing between the roles played by the dielectric and by the plasma. Section III describes our geometry: screening in a semi-infinite medium. Section IV considers source charge in the vacuum. Section V considers source charge in the semiconductor. Section VI considers source charge on the surface, emphasizing the surface potential ϕ_s at large and intermediate distances; at large distances it is quadrupolar (an inverse cube potential), but for intermediate distances it is indeed well approximated by Eq. (1). The theory predicts that R_s is the bulk screening length R_b, consistent with the modulation of STM contours by individual defects, but not with the much shorter screening length inferred in Ref. 3. We discuss a possible reason for this discrepancy in Sec. VII, where we apply the theory of Sec. VI to the results of Ref. 3. Section VIII presents a summary.

II. OVERVIEW OF BULK SCREENING

For later purposes of comparison with our results in the presence of a surface, we review screening by an infinite medium within the Debye-Hückel (or, equivalently, the Thomas-Fermi) approximation.[4,5] Consider an infinite conducting medium of relative dielectric constant ε due to electrons in bound orbitals, and possessing a density n of free carriers (of either sign) with delocalized orbitals. If the temperature T is sufficiently high that the free carriers nearly satisfy the Maxwell-Boltzmann distribution, then Debye-Hückel theory applies, and the density of states is given by $\partial n/\partial\mu \approx k_B T/n$, where μ is the chemical potential of these carriers, and k_B is Boltzmann's constant. If the temperature T is sufficiently low that the free carriers nearly satisfy the Fermi-Dirac distribution, then Thomas-Fermi theory applies, and $\partial n/\partial\mu \approx (3/2)(n/\mu)$. Within Debye-Hückel theory, for a point charge q embedded in such a system, the electrical potential ϕ at distance r from the source is given by

$$\phi(r) = \frac{q}{4\pi\varepsilon_0\varepsilon r}\exp(-r/R_b), \quad R_b \equiv \sqrt{\frac{\varepsilon\varepsilon_0 k_B T}{ne^2}}. \qquad (2)$$

If Fermi-Dirac, rather than Maxwell-Boltzmann statistics apply, then the ratio $k_B T/n$ is replaced by $\partial\mu/\partial n$.[4,5] In Eq. (2) the dielectric constant ε appears twice for the following reasons. First, atomic and molecular polarization due to localized states, in response to the presence of q, gives a factor of $1/\varepsilon$ in the potential near q. Second, polarization charge also screens the free carriers, making their screening less effective, and thereby increasing the screening length by a factor $\sqrt{\varepsilon}$. Thus $R_b = R_b^{(0)}\sqrt{\varepsilon}$, where $R_b^{(0)}$ is the Debye-Hückel screening length for $\varepsilon = 1$. It is implicit that $R_b > a$.

Figure 1 gives a qualitative picture of screening for a spherical sample with a source charge q at its center. The total charge response near the source has two contributions: (1) within a of the source q, there is an induced polarization charge of $-q(1-1/\varepsilon)$, yielding an effective source charge of q/ε; (2) within a few R_b of the effective source charge q/ε there is a screening charge $-q/\varepsilon$, of which $q(1-1/\varepsilon)$ is due to polarization, and $-q$ is due to free carriers. In order to satisfy charge conservation there are, in addition, two more contributions at the (distant) surface of the sample; (3) within a few times R_b of the surface there is a screening charge q/ε, where $-q(1-1/\varepsilon)$ is due to polarization, and q is due to free carriers; (4) within an atomic distance of the surface there is an induced polarization charge of $q(1-1/\varepsilon)$. The sum of all induced free charge is zero, the sum of all polarization charge within a few screening lengths of the source is zero, and the sum of all the polarization charge within a few screening lengths of distant surfaces is zero.

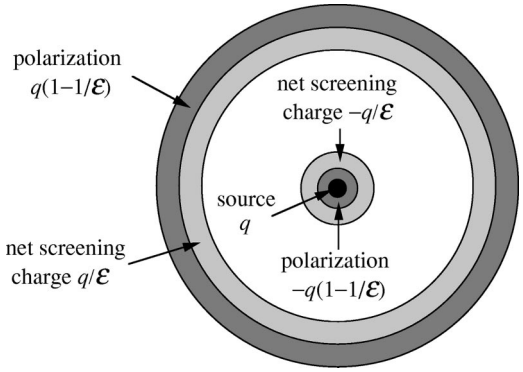

FIG. 1. Semiconductor screening for a source charge q within a spherical sample. The light hatching represents exponential screening over the length R_b; the dark hatching represents screening over an atomic distance a.

III. GEOMETRY OF THE PROBLEM

For a semi-infinite semiconductor in contact with vacuum, we consider the following geometry: the region $z>0$ contains vacuum, with dielectric constant $\varepsilon = 1$ and the region $z<0$ contains semiconductor, with dielectric constant ε; thus, the $z=0$ plane defines their interface. The point charge q is on the z axis at $\mathbf{r}_0 = (0,0,z_0)$, as shown in Fig. 2.

In the sections to follow, we consider all three possibilities for the source charge q: q in the vacuum region ($z_0 > 0$), q within the semiconductor ($z_0 < 0$), and q at the vacuum-semiconductor interface ($z_0 = 0$).

For a source charge on the surface, we expect a dipole potential (inverse square) at large distances. The dipole occurs because, although the screening charge is equal and opposite to the source charge, it is spread out within the bulk of the semiconductor. Along the surface, however, this dipole potential vanishes, leaving a dominant quadrupole potential (inverse cube). Nevertheless, as shown in Eq. (35) below, at

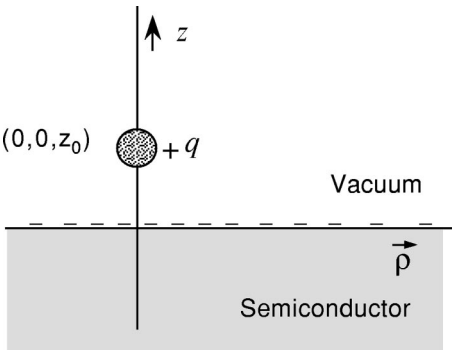

FIG. 2. Geometry for a source q in vacuum, including the electrostatic response of the semiconductor.

intermediate distances the exponential form (2) applies, with r replaced by ρ and the effective charge q/ε replaced by $2q/\varepsilon$.

IV. ELECTROSTATIC SCREENING FOR SOURCE CHARGE IN THE VACUUM

When q is in the vacuum region, its volume charge density, expressed in cylindrical coordinates, is

$$\rho_b = q\,\delta(\mathbf{r}-\mathbf{r}_0) = \frac{q}{2\pi}\frac{\delta(\rho)}{\rho}\delta(z-z_0). \tag{3}$$

Thus, Poisson's equation[6] for the electrostatic potential in the vacuum ϕ_v is

$$\nabla^2\phi_v = -\frac{q}{\varepsilon_0}\delta(\mathbf{r}-\mathbf{r}_0) \quad (z>0). \tag{4}$$

The electrostatic potential ϕ_b in the semiconductor bulk, when there is no source charge, must satisfy

$$\nabla^2\phi_b = -\frac{\rho_{free}}{\varepsilon\varepsilon_0}, \quad (z<0), \tag{5}$$

where ρ_{free} is the charge density due to free carriers. In Debye-Hückel theory, ρ_{free} is related to ϕ_b by

$$\rho_{free} = -\varepsilon\varepsilon_0 k_b^2\phi_b, \quad k_b \equiv R_b^{-1}. \tag{6}$$

Here k_b is the inverse of the bulk screening length R_b, given in Eq. (2). From Eq. (6), and a knowledge of ϕ_b, ρ_b can be deduced. Employing Eq. (6) in Eq. (5), we see that ϕ_b satisfies

$$\nabla^2\phi_b - k_b^2\phi_b = 0 \ (z<0). \tag{7}$$

The solution for ϕ_v is a superposition[6] of two terms: $\phi_v^{(1)}$, which satisfies Eq. (4); and $\phi_v^{(2)}$, which satisfies Laplace's equation $\nabla^2\phi_v^{(2)}=0$. Because the system has axial symmetry, all physical quantities are independent of the polar angle φ. Hence, the solutions of the electrostatic equations can be expanded in terms of the zeroth order Bessel function. Thus (see the Appendix),

$$\phi_v = \frac{q}{4\pi\varepsilon_0}\int_0^\infty dk\, J_0(k\rho)[\exp(-k|z-z_0|) + C_v(k)\exp(-kz)] \quad (z>0). \tag{8}$$

The solution for ϕ_b similarly can be written as

$$\phi_b = \frac{q}{4\pi\varepsilon_0}\int_0^\infty dk\, D_b(k) J_0(k\rho)\exp(z\sqrt{k^2+k_b^2}) \quad (z<0). \tag{9}$$

The unknown functions $C(k)$ and $D(k)$ are determined by matching the tangental component of **E** and normal component of **D** at the vacuum-semiconductor interface $z=0$ where

$$\frac{\partial\phi_v}{\partial\rho} = \frac{\partial\phi_b}{\partial\rho} \text{ and } \frac{\partial\phi_v}{\partial z} = \varepsilon\frac{\partial\phi_b}{\partial z}. \tag{10}$$

Use of Eq. (10) in Eqs. (8) and (9) yields

$$C_v(k) = \frac{k-\varepsilon\sqrt{k^2+k_b^2}}{k+\varepsilon\sqrt{k^2+k_b^2}}\exp(-kz_0) \text{ and}$$

$$D_b(k) = \frac{2k}{k+\varepsilon\sqrt{k^2+k_b^2}}\exp(-kz_0). \tag{11}$$

Related expressions were derived in an earlier study that emphasized image effects on tunneling through metal-vacuum-semiconductor junctions.[7]

A. Bulk and vacuum potentials

Within the semiconductor, $D_b(k)$ in Eq. (11) determines the behavior of ϕ_b in Eq. (9). There are two characteristic lengths in $D_b(k)$. One is $k_b^{-1}=R_b$, and the other is z_0.

For $R_b \ll z_0$, corresponding to relatively strong metallic screening, the factor $\exp(-kz_0)$ is already very small before the denominator in $D_b(k)$ displays any significant k dependence. Hence we can write $D_b(k)\approx(2k/\varepsilon_0 k_b)\exp(-kz_0)$. Then, for $z<0$, use of Eq. (6.623.2) from Ref. 8 in Eq. (9) yields

$$\phi_b = \frac{q}{4\pi\varepsilon_0}\int_0^\infty dk\frac{2k}{\varepsilon k_b}\exp(-kz_0)J_0(k\rho)\exp(-k_b|z|)$$

$$= \frac{qz_0R_b\exp(-|z|R_b)}{2\pi\varepsilon\varepsilon_0(z_0^2+\rho^2)^{3/2}} \ (R_b \ll z_0, z<0). \tag{12}$$

As expected in the limit of an ideal metal, for $z=0$, $\phi_b \to 0$ as $R_b \to 0$. For $\varepsilon=1$, Eq. (12) is in agreement with a recent work that considers only the case $R_b \ll z_0$ and $\varepsilon=1$.[9]

We now turn to some numerical results, presented for the source q both near ($z_0=0.1R_b$) and far ($z_0=10R_b$) from the surface, and for the observer both near ($|z|=0.1R_b$) and far ($z_0=10R_b$) from the surface. In all of our calculations, the distances ρ and z are in units of $k_b^{-1}\equiv R_b$ (the bulk screening length), and the potentials are in units of

$$\phi_0 \equiv \frac{q}{4\pi\varepsilon_0 R_b}, \tag{13}$$

the potential in vacuum at a distance R_b from the bare source charge. We take $\varepsilon=10$ as typical of many semiconductors. R_b is nonzero and finite. If R_b were infinite, the semiconductor would behave like a dielectric (no free charge in the semiconductor bulk). If R_b were zero, by Eqs. (9) and (11) the semiconductor would behave like an ideal metal. For both of these limits, the electrostatic potentials have well-known, analytical solutions.[6]

Figures 3–6 give the potentials $\phi_v^{V,D,M,S}$ in vacuum (v) and $\phi_b^{V,D,M,S}$ in bulk (b) when the lower half-space is occupied by vacuum (V), dielectric with $\varepsilon=10$ (D), ideal metal (M), or a semiconductor (S) with $\varepsilon=10$.

Figure 3 gives the potentials in vacuum for small $z_0=z=0.1R_b$ (source and observer both near the surface). For small ρ, ϕ_v^S approaches ϕ_v^D. However, ϕ_v^S falls rapidly for large ρ, due to screening by bulk charge. As expected, ϕ_v^S lies between ϕ_v^D and the potential ϕ_v^M for the ideal metal. The drastic difference between ϕ_v^V and ϕ_v^D shows that the dominant role in screening at small z_0 is due to surface po-

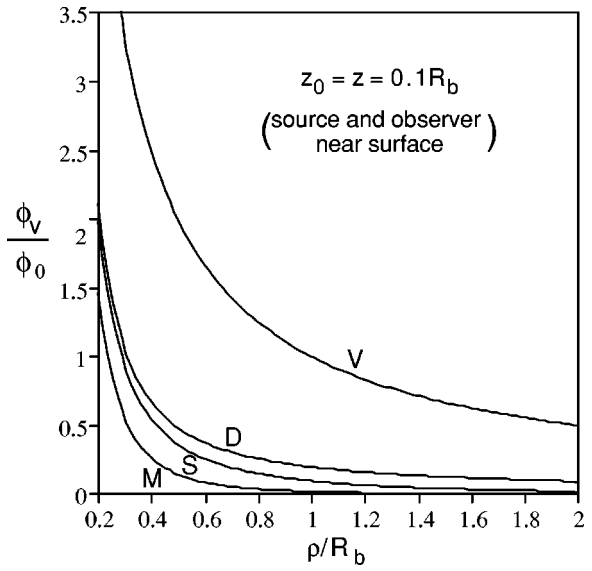

FIG. 3. Electrostatic potential in the vacuum ($z>0$), for a source charge in vacuum and source and observer near the surface; $z_0=z=0.1R_b$. The legend is *V* (vacuum), *D* (dielectric), *S* (semiconductor), and *M* (metal).

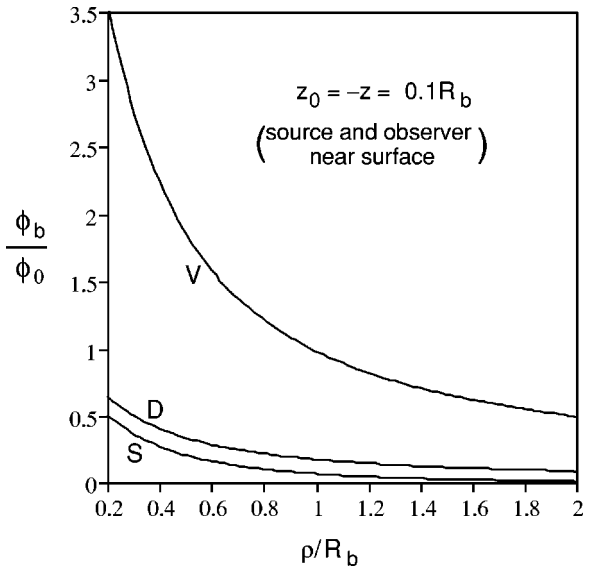

FIG. 5. Electrostatic potential within the bulk medium ($z<0$), for a source charge q in vacuum and source and observer near the surface; $z_0=-z=0.1R_b$. The legend is *V* (vacuum), *D* (dielectric), and *S* (semiconductor).

larization charge. Bulk charge has an important role for larger radial distances from q.

Figure 4 shows the potentials in vacuum for large $z_0=z=10R_b$ (source and observer both far from the surface). For $z<0$, ϕ_v^S approaches ϕ_v^M, and ϕ_v^0 is slightly greater than ϕ_v^S. This again indicates that for q far from the surface, the metallic properties of the semiconductor dominate the screening.

Similar behavior is seen in Fig. 5 and Fig. 6 for the potentials in bulk (the lower half-space $z<0$). The ideal metal potential ϕ_b^M is not shown, being trivially zero in this case.

In principle, the value of ε at the surface could differ from its value in bulk. This easily can be incorporated into the present theory if it appears necessary, by suitably modifying Eq. (10).

B. Surface and bulk charge distribution

We first consider the surface charge distribution σ_s at the surface $z=0$. This is found from

$$\sigma_s=\varepsilon_0\left[-\frac{\partial\phi_v}{\partial z}+\frac{\partial\phi_b}{\partial z}\right]_{z_0=0}=-(\varepsilon-1)\varepsilon_0\left.\frac{\partial\phi_b}{\partial z}\right|_{z_0=0}. \tag{14}$$

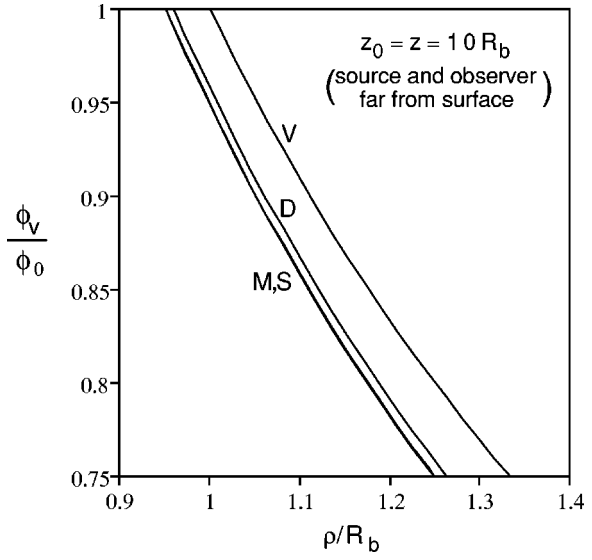

FIG. 4. Electrostatic potential in the vacuum ($z>0$), for a source charge in vacuum and source and observer far from the surface; $z_0=z=10R_b$. The legend is *V* (vacuum), *D* (dielectric), *S* (semiconductor), and *M* (metal).

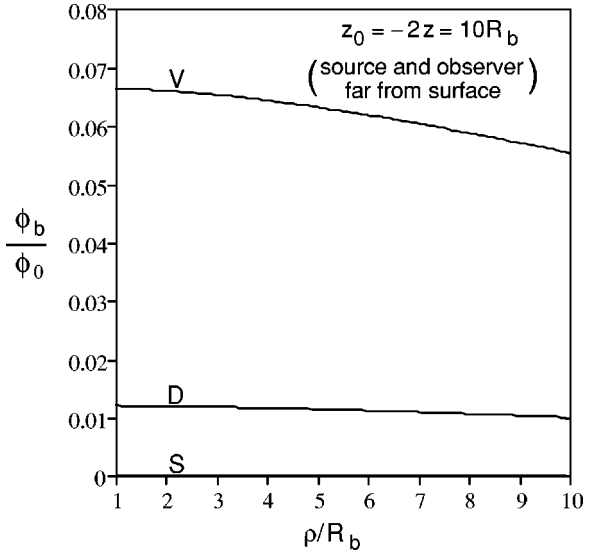

FIG. 6. Electrostatic potential within the bulk medium ($z<0$), for a source charge q in vacuum and source and observer far from the surface; $z_0=-2z=10R_b$. The legend is *V* (vacuum), *D* (dielectric), and *S* (semiconductor).

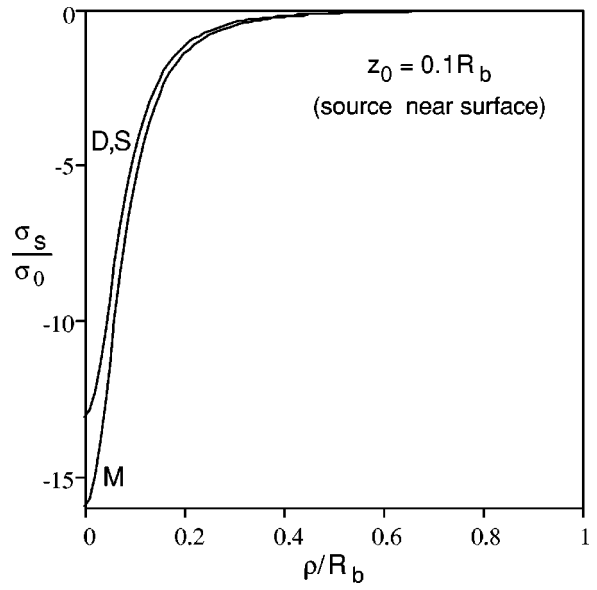

FIG. 7. Surface charge distribution for a source charge q in vacuum and near the surface; $z_0=0.1R_b$. The legend is D (dielectric), S (semiconductor), and M (metal).

From the solution for ϕ_b, we obtain

$$\sigma_s=-\frac{q}{2\pi}(\varepsilon-1)\int_0^\infty dk\,J_0(k\rho)\frac{k\sqrt{k^2+k_b^2}}{k+\varepsilon\sqrt{k^2+k_b^2}}\exp(-kz_0). \tag{15}$$

It appears that the integral in Eq. (15) cannot be evaluated analytically,[8] so we evaluate it numerically.[10]

Figures 7 and 8 show σ_s normalized to $\sigma_0\equiv q/R_b^2$ when q is near and far from the interface. For small z_0, as shown in Fig. 7, σ_s is very similar to the surface charge distribution in the vacuum-dielectric case. Also, σ_s differs from the distribution on an ideal metal surface only for very small ρ ($\rho<0.5R_b$). This is because the entire response is localized radially. For an ideal metal, where there is no smallest characteristic dimension, electrostatic induction brings free charge literally to the surface. This free charge completely screens the source charge q for $z<0$. For a semiconductor, on the other hand, where the smallest characteristic dimension is an atomic dimension a, the only charge literally on the surface is the polarization charge associated with the topmost atoms. This polarization charge performs only partial screening.

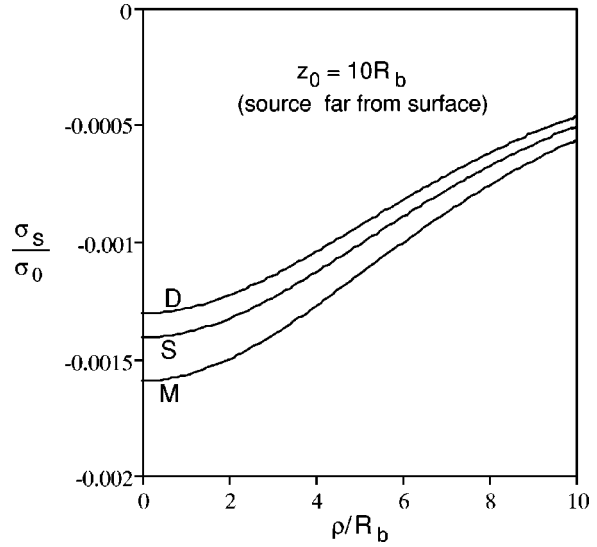

FIG. 8. Surface charge distribution for a source charge q in vacuum and far from the surface; $z_0=10R_b$. The legend is D (dielectric), S (semiconductor), and M (metal).

Figure 8 considers large z_0. As q moves further from the surface, the dielectric, ideal metal, and semiconductor curves become more distinct and more smooth. In that case, q affects a much greater area, and the induced charge is smeared out along the surface.

The total induced surface charge q_s is given by

$$q_s=2\pi\int_0^\infty d\rho\,\rho\sigma_s(\rho). \tag{16}$$

Placing Eq. (16) into Eq. (15) yields an expression that can be evaluated analytically in the two limits $z_0\ll R_b$ and $z_0\gg R_b$ (see the Appendix).

For $z_0\ll R_b$, Eq. (A22) yields

$$q_s=-q\frac{\varepsilon-1}{\varepsilon+1}\ (z_0\ll R_b). \tag{17}$$

This q_s equals the induced charge for the vacuum-dielectric case,[6] supporting the conclusion that, for small z_0, the dielectric properties of the semiconductor dominate. In fact, we find numerically that, as z_0 decreases, ϕ_v and ϕ_b shift toward the corresponding potentials for the vacuum-dielectric case. Thus the curves for semiconductor and dielectric nearly coincide in Fig. 5.

For $z_0\gg R_b$, Eq. (A24) yields

$$q_s=-q\frac{\varepsilon-1}{\varepsilon}=-q\left(1-\frac{1}{\varepsilon}\right)\ (z_0\gg R_b). \tag{18}$$

Here the metallic properties of the semiconductor again dominate (for an ideal metal $R_b\to 0$, so we have $z_0\gg R_b$ for all finite z_0). The value for q_s, and the form of σ_s, can be obtained in this case by the following physical argument. If the electric field lines are orthogonal to the $z=0$ plane, then the boundary condition for the dielectric displacement $\mathbf{D}$ gives $D_v=\varepsilon_0E_v=D_b=\varepsilon_0\varepsilon E_b$. The boundary condition for the electric field $\mathbf{E}$ at $z=0$ then becomes

$$\sigma_s=\varepsilon_0(\mathbf{E}_v-\mathbf{E}_b)\cdot\mathbf{e_z}=\varepsilon_0\frac{\varepsilon-1}{\varepsilon}\mathbf{E_v}\cdot\mathbf{e_z}, \tag{19}$$

where $\mathbf{e_z}$ is a unit vector in the z direction. Applying Gauss's law and Gauss's theorem, with $d\mathbf{S}=-dS\mathbf{e_z}$, we obtain

$$q_s=\oint\sigma^S dS=-\varepsilon_0\frac{\varepsilon-1}{\varepsilon}\oint\mathbf{E_v}\cdot d\mathbf{S}$$

$$=-\varepsilon_0\frac{\varepsilon-1}{\varepsilon}\int\nabla\cdot\mathbf{E_v}dV=-q\left(1-\frac{1}{\varepsilon}\right), \tag{18'}$$

as in Eq. (18) above.

We now consider the bulk charge distribution ρ_b. Within the semiconductor ($z<0$), following Eq. (6), both the free charge distribution ρ_{free} and the polarization charge distribution $\rho_{pol}=\rho_{free}(-1+\varepsilon^{-1})$ vary linearly with ϕ_b. It turns out that the bulk charge densities are localized within a few R_b of the surface, for both large and small z_0. For small z_0, the charge distribution is also localized radially, whereas for large z_0, the charge distribution is extended radially.

From q_s for both small and large z_0, we see that q is not immediately screened at the surface. The effective source charge Q seen by the bulk is

$$Q=q+q_s>0, \tag{20}$$

and this is screened by the bulk. Charge conservation applied to the entire system $[z\in(-\infty,\infty)]$ implies that there is also charge near and on the boundary at infinity.

For $z_0\ll R_b$, by Eqs. (20) and (17) Q is given by

$$Q=q-q\frac{\varepsilon-1}{\varepsilon+1}=\frac{2q}{1+\varepsilon}\quad(z_0\ll R_b). \tag{21}$$

Therefore, the total screening charge q_b in the semiconductor, within a few R_b of the surface, is $q_b=-Q=-2q/(1+\varepsilon)$. Using

$$q_b=q_{free}+q_{pol},\quad \frac{q_b}{\varepsilon}=q_{free},\quad (z_0\ll R_b) \tag{22}$$

the total free and polarization charge in the semiconductor are

$$q_{free}=-\varepsilon Q=-2q\frac{\varepsilon}{1+\varepsilon},\qquad q_{pol}=-Q-q_{free}=2q\frac{\varepsilon-1}{1+\varepsilon}. \tag{23}$$

For $z_0\gg R_b$, by Eqs. (20) and (18) Q is given by

$$Q=q-q\frac{\varepsilon-1}{\varepsilon}=\frac{q}{\varepsilon}\quad(z_0\gg R_b). \tag{24}$$

Therefore

$$q_{free}=-\varepsilon Q=-q,\quad q_{pol}=-Q-q_{free}=q\frac{\varepsilon-1}{\varepsilon}. \tag{25}$$

For $z_0\ll R_b$, the free charge at infinity is $2q\varepsilon/(1+\varepsilon)$, and the polarization charge is $q(\varepsilon-1)/(\varepsilon+1)$. However, for $z_0\gg R_b$, there is at infinity a deficiency $+q$ of free charge and no residual polarization charge.

V. ELECTROSTATIC SCREENING FOR SOURCE CHARGE WITHIN THE SEMICONDUCTOR

When the source charge q is within the semiconductor (Fig. 9), the physical picture differs significantly from that for a source charge in the vacuum (Fig. 2). For q positive, a negative polarization charge is induced near q in the bulk. Further from q are both free and polarization charge distributions. The semiconductor surface now has a positive polarization charge, in contrast to the negative surface polarization charge for the source in vacuum. This is because in the limit $k_b\to 0$, where the semiconductor behaves like a dielectric (with no polarization volume charge density), negative charge induced near q leaves a positively charged interface (Fig. 9).

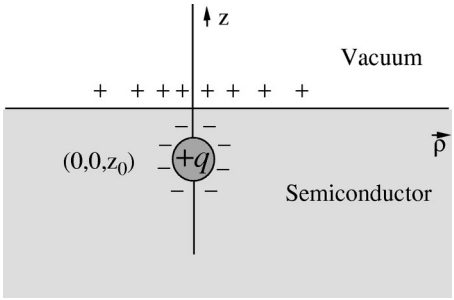

FIG. 9. Electrostatic response of a semiconductor to a source charge q within it.

The potential in vacuum now satisfies Laplace's equation $\nabla^2\phi_v=0$, whereas ϕ_b now satisfies

$$\nabla^2\phi_b-k_b^2\phi_b=-\frac{1}{\varepsilon\varepsilon_0}q\,\delta(\mathbf{r}-\mathbf{r}_0)=-\frac{1}{\varepsilon\varepsilon_0}\frac{q}{2\pi}\frac{\delta(\rho)}{\rho}\delta(z-z_0)\quad(z<0). \tag{26}$$

Solving these equations (see the Appendix), one obtains

$$\phi_v=\frac{q}{4\pi\varepsilon_0}\int_0^\infty dk\,C_v(k)J_0(k\rho)\exp(-kz)\quad(z>0), \tag{27}$$

$$\phi_b=\frac{q}{4\pi\varepsilon_0}\int_0^\infty dk\,J_0(k\rho)\left(\frac{k}{\varepsilon\sqrt{k^2+k_b^2}}\exp(-\sqrt{k^2+k_b^2}|z-z_0|)+D_b(k)\exp(z\sqrt{k^2+k_b^2})\right). \tag{28}$$

From the boundary conditions on $\mathbf{D}$ and $\mathbf{E}$ at the $z=0$ plane, $C(k)$ and $D(k)$ are given by

$$C_v(k)=\frac{2k}{k+\varepsilon\sqrt{k^2+k_b^2}}\exp(-\sqrt{k^2+k_b^2}|z_0|), \tag{29}$$

$$D_b(k)=\left(\frac{2k}{k+\varepsilon\sqrt{k^2+k_b^2}}-\frac{k}{\varepsilon\sqrt{k^2+k_b^2}}\right)\exp(-\sqrt{k^2+k_b^2}|z_0|). \tag{30}$$

Applying Eq. (14) to the solution given by Eqs. (28) and (30), the surface charge distribution is

$$\sigma_s=\frac{q}{2\pi}\frac{\varepsilon-1}{\varepsilon}q\int_0^\infty dk\,J_0(k\rho)\frac{k^2}{k+\varepsilon\sqrt{k^2+k_b^2}}\times\exp(-|z_0|\sqrt{k^2+k_b^2}). \tag{31}$$

If $R_b\to\infty$, Eq. (31) reduces to the surface charge distribution due to q in a semi-infinite dielectric[6]

$$\sigma_d=\frac{q}{2\pi}\frac{\varepsilon-1}{\varepsilon(\varepsilon+1)}\frac{|z_0|}{\sqrt{\rho^2+|z_0|^2}^3}>0 \quad (z_0<0, R_b\to\infty). \tag{32}$$

Note that Eq. (31) cannot give the surface charge distribution (due to polarization) for $z_0=0$ in the limit $z_0\to 0^-$. This is because as soon as q is moved into the semiconductor, negative polarization charge is induced near q, leaving positive polarization charge on the surface. (This apparent discontinuity is a consequence of the theory not depending explicitly on atomic size.) On the other hand, as we shall see below, the surface charge distribution for $z_0\to 0^+$, from Eq. (14), approaches the corresponding distribution for $z_0=0$, due to the absence of an intrinsic charge distribution in the vacuum. As shown following Eq. (A22), Eq. (31) can be integrated exactly, yielding the total surface charge in the vacuum-dielectric case $(R_b\to\infty)$[6]

$$q_s=q\frac{\varepsilon-1}{\varepsilon(\varepsilon+1)} \quad (z_0<0,\ R_b/|z_0|\to\infty). \tag{33}$$

This charge is due solely to polarization. We conclude that the dielectric properties of the semiconductor dominate for small z_0 even when the source is within the semiconductor. The free and polarization charges in the bulk are, in this limit, the same as for $z_0>0$.

We now turn to the bulk charge. Within an atomic distance a of q itself is a polarization charge $-q(1-1/\varepsilon)$, yielding a net charge of q/ε. Since the system will be locally neutral within a few R_b of q, the total nearby bulk charge q_b is given by $q_b=-(q/\varepsilon+q_s)=-2q/(1+\varepsilon)$. Of this, $-2q/\varepsilon(1+\varepsilon)$ is free charge and $-2q(\varepsilon-1)/\varepsilon(1+\varepsilon)$ is polarization charge. Near and on the boundary at infinity, there is a net charge q. Of this, $2q/\varepsilon(1+\varepsilon)$ is free charge equal to the negative of the free charge near the source q, and there is an associated bulk polarization charge given by $2q(\varepsilon-1)/\varepsilon(1+\varepsilon)$; there is also a surface polarization charge of $q(\varepsilon-1)/(\varepsilon+1)$. The sum of the free charge is zero, as is the sum of the polarization charge (both bulk and volume). Although the detailed distribution of surface polarization charges is different in the two cases, here the sum of the surface polarization charges at the interface and at infinity is $q(1-1/\varepsilon)$, the same as for the spherical geometry of Fig. 1.

For the source far inside the semiconductor $(z_0<0, |z_0|\gg R_b)$, Eq. (31) implies that q_s approaches zero so the system behaves as if there is no vacuum-semiconductor interface. Thus, in this limit $\phi_v\to 0$ whereas ϕ_b approaches Eq. (2), the solution for the infinite semiconductor case, with r replaced by $\sqrt{\rho^2+|z-z_0|^2}$.

VI. ELECTROSTATIC SCREENING FOR SOURCE CHARGE ON THE SURFACE

When q is at the vacuum-semiconductor interface $(z_0=0^+)$, the electrostatic potentials ϕ_v and ϕ_b can be obtained from Eqs. (8), (9), and (11), in the limit $z_0\to 0^+$. Their functional behavior is similar to those for $z_0>0$ with $z_0\ll R_b$: for small ρ (up to $1.0R_b$) and close to the interface, both ϕ_v and ϕ_b behave like the corresponding potentials ϕ_v^D and ϕ_b^D in the vacuum-dielectric case. However, as ρ increases, the potentials decrease more rapidly due to the induced bulk charge localized near the surface. When z is large, the difference between ϕ_v and ϕ_v^D, and between ϕ_b and ϕ_b^D, is significant for all ρ. The potential ϕ_b becomes negligible compared with ϕ_b^D, due to plasma screening by the semiconductor. The potential ϕ_v is also suppressed compared with ϕ_v^D, due to its dependence on $z+z_0$. (Its behavior for large z and $z_0=0^+$ is similar to the behavior for finite z and large z_0, where, as discussed earlier, the semiconductor's metallic properties dominate.)

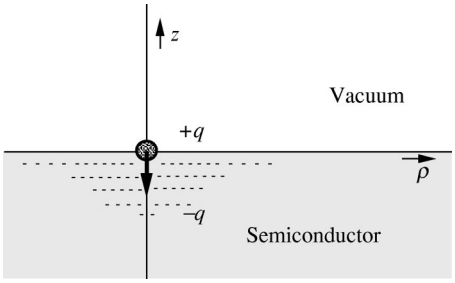

FIG. 10. For $z_0=0$, the total charge distribution has a dipole and a quadrupole moment. At large distances along the surface, the dipole potential is zero, and the quadrupole potential dominates. The arrow indicates the centroid of the induced bulk charge.

The induced surface charge density for $z_0=0^+$ is singular at $\rho=0$, and zero for all $\rho>0$. It is similar to that in the vacuum-dielectric case,[6] where $\sigma_d(z_0=0^+)\sim 1/\rho^3$. The total charge Q on the surface is the sum of q and the polarization charge q_s of Eq. (17), so $Q=2q/(1+\varepsilon)$, as in Eq. (21). Thus the total bulk charge near the surface is $-2q/(1+\varepsilon)$. A schematic picture of the charge induced in the semiconductor is shown in Fig. 10. Negative polarization charge is induced at the surface, in response to positive q. The source q is partially screened by this surface polarization charge, and the remainder is completely screened by free charge in the bulk. This bulk charge is localized near the z axis, extending a few R_b into the semiconductor.

The potential on the surface $\phi_s(\rho)$ is relevant to the interaction between charged surface defects. Setting $z=0$ and $z_0=0$ in Eqs. (8) and (11) gives

$$\phi_s=\frac{q}{4\pi\varepsilon_0}\int_0^\infty dk\, J_0(k\rho)\frac{2k}{k+\varepsilon\sqrt{k^2+k_b^2}}. \tag{34}$$

Although Eq. (34) has no general analytical solution, it can be approximated in the two limits of small and large ρ. The small ρ limit may be obtained analytically only for dielectric constant $\varepsilon\gg 10$. The large ρ limit may be obtained analytically for all ε.

If $\varepsilon\gg 10$, the integrand of Eq. (34) can be approximated by $J_0(k\rho)(2k/\varepsilon\sqrt{k^2+k_b^2})$, which can be integrated analytically[8] to give

$$\phi_s\cong\frac{q}{4\pi\varepsilon_0}\int_0^\infty dk\, J_0(k\rho)\frac{2k}{\varepsilon\sqrt{k^2+k_b^2}}=\frac{2q}{4\pi\varepsilon_0\varepsilon}\frac{\exp(-k_b\rho)}{\rho}$$

$$=\frac{2q}{4\pi\varepsilon_0\varepsilon}\frac{\exp(-k_{b_0}\sqrt{\varepsilon}\rho)}{\rho}\ (\varepsilon\gg 1, \rho\ll 4R_b), \tag{35}$$

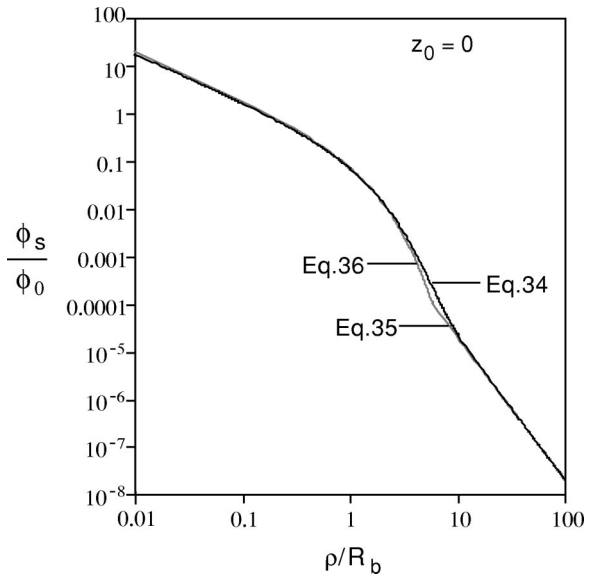

FIG. 11. Surface potential for a source charge on the surface ($z_0=0$), and its two limits for small and large ρ. Note the logarithmic scales along both axes.

where $k_{b_0}^{-1}=R_b^{(0)}$. By Eq. (35), for small radial separations, $\phi_s(\rho)$ is similar to the potential $\phi(r)$ in Eq. (2) for an infinite semiconductor. The only difference is in the effective charge, which for the semi-infinite case is twice as large.

Let us now consider the large ρ limit, for any ε. From Eq. (A18) of the Appendix, the surface potential $\phi_s=\phi(z=0,\rho)$ for large ρ has the form

$$\phi_s(\rho)=\frac{1}{4\pi\varepsilon_0}\frac{2R_b^2}{\varepsilon^2}\frac{q}{\rho^3} \quad (\rho\gg 8R_b). \tag{36}$$

Equations (34)–(36) are plotted in Fig. 11, for $\varepsilon=10$.

Equation (36) has a natural interpretation in terms of a multipole expansion of the potential, since all of the charge lies within a few screening lengths of the source charge q. An inverse cube in the potential corresponds to a quadrupole potential.[6] The inverse first power is absent because the source charge is completely screened by charge in the semiconductor. The inverse second power is absent because the dipole moment **p** lies along the z axis, and thus is normal to a radius vector **r** from the source charge q at the origin to an observer elsewhere along the surface. That is, the dipole potential

$$\phi_{dipole}(\mathbf{r})=\frac{1}{4\pi\varepsilon_0}\frac{\mathbf{p}\cdot\mathbf{r}}{r^3}, \tag{37}$$

gives zero for $\mathbf{r}=\vec{\rho}$. The next term is the quadrupole potential,[6]

$$\phi_{quadrupole}(\mathbf{r})=\frac{1}{4\pi\varepsilon_0}\sum_{ij}\frac{Q_{ij}x_ix_j}{2r^5}, \tag{38}$$

where x_i is the i component of **r**, and the quadrupole tensor is

$$Q_{ij}=\int d\mathbf{r}'\rho(\mathbf{r}')(3x_i'x_j'-r'^2\delta_{ij}). \tag{39}$$

For a system with axial symmetry about the z axis, Q_{ij} has no off-diagonal elements, and $Q_{xx}=Q_{yy}$. Also, by the traceless nature of Q_{ij}, $Q_{zz}=-2Q_{xx}$. Hence there is only one independent term in Q_{ij}. We find Q_{xx} for the present system by comparing Eq. (36) with Eq. (38). This yields

$$Q_{xx}=Q_{yy}=-\frac{1}{2}Q_{zz}=\frac{4}{\varepsilon^2}qR_b^2. \tag{40}$$

In the present case, where there is a nonzero dipole moment **p** (to be determined shortly), the definition of the quadrupole tensor depends upon the choice of origin.[6] Here **p** points upward for positive q; we take it to have magnitude p. If we were to choose as our origin another point at a distance d below the surface, the dipole potential on the surface would be $pd/4\pi\varepsilon_0\rho^3$. However, on using the redefined quadrupole moments ($Q_{xx}\rightarrow Q_{xx}-2pd$), the overall potential would still satisfy Eq. (36).

To evaluate the dipole moment we find the potential for $z\gg R_b$ and $\rho=0$, where Eq. (8) applies. Setting $z_0=0$ and $J(0)=1$ in Eq. (8), and using Eq. (11), we find that

$$\phi_v=\frac{q}{4\pi\varepsilon_0}\int_0^\infty dk\frac{2k}{k+\varepsilon\sqrt{k^2+k_b^2}}\exp(-kz) \quad (z>0). \tag{41}$$

In the limit where $k_bz\gg 1$, this becomes

$$\phi_v=\frac{q}{4\pi\varepsilon_0}\int_0^\infty dk\frac{2k}{\varepsilon k_b}\exp(-kz)=\frac{1}{4\pi\varepsilon_0}\frac{2qR_b}{\varepsilon z^2}\ (k_bz\gg 1), \tag{42}$$

Comparison with Eq. (37) evaluated for $\rho=0$ leads to a dipole moment of magnitude

$$p=\frac{2qR_b}{\varepsilon}. \tag{43}$$

There are two ways to interpret this dipole moment in terms of a charge and a length. On the one hand, the dipole in Eq. (43) can be thought of as being due to q at the origin and $-q$ at a distance $l=p/q=2R_b/\varepsilon$ below the origin. On the other hand, it also can be thought of as due to $q+q_s=2q/(\varepsilon+1)$, where q_s is due to surface polarization charge around the source q and $-(q+q_s)$ at a distance $l'=p/(q+q_s)=R_b(\varepsilon+1)/\varepsilon$ below the origin. This latter definition includes only the effects of free charge and of bulk polarization charge. For $z_0\neq 0$, there is an additional dipole moment $2qz_0$, due to the source charge at z_0 and its classical image $-q$ at $-z_0$, as can be shown explicitly from Eqs. (8) and (11). (Because $z\gg R_b$, metallic screening dominates.)

It is worth mentioning in passing that these results are also relevant to the interaction of two colloidal particles on a surface. This situation recently has been studied in Ref. 11. There the authors treat the system as if the background fluid (typically water, with dielectric constant near 80) can be treated by working out the results for dielectric constant unity and then scaling to include the dielectric constant. In particular, although they employ Eq. (26), they do not employ Eqs. (10) or (14). As a consequence, their elegant result

for the surface potential due to a colloid on the surface is valid only for $\varepsilon=1$. Because our focus is on the semiconductor case, we do not develop, here, the implications of Eq. (34) for colloids.

VII. COMPARISON WITH EXPERIMENT

Equation (35) shows that the exact ϕ_s of Eq. (34) is well approximated by a screened exponential with a surface screening length equal to the bulk screening length R_b. This result provides a rigorous basis for the ansatz of an exponentially decaying envelope, with characteristic length R_b, commonly employed to analyze STM images of the depletion or accumulation regions surrounding isolated charges (i.e., the dilute limit) on III–V(110) cleavage surfaces.[2]

We turn now to the more detailed and explicit results of Ref. 3, which concern the potential itself, not merely its dominant spatial variation. (These results are obtained for a surface-charge concentration that is much larger than in Ref. 2.)

Reference 3 describes a room-temperature STM determination of the pair correlation function for positively charged phosphorous vacancies at the (110) surface of *p*-type InP. The vacancies were created by *in vacuo* thermal anneals at 100–200 °C. The interaction energy $U(\rho)$, between two vacancies a distance ρ apart, was obtained from the logarithm of the pair correlation function and scaled to the annealing temperature. As noted in the Introduction, the results were satisfactorily fit by Eq. (1) with $|q|=(1)e$, $\varepsilon_{eff}=(\varepsilon+1)/2$, and $R_s=1.1$ nm.

To compare the present linearized theory with the experiments of Ref. 3, we first note that in the linear regime the electrostatic interaction between two surface charges q and q_0 is $U=q_0\phi_s(\rho)$, where $\phi_s(\rho)$ is the surface potential at separation ρ due to the charge q at the origin.[12] Equation (35) shows this interaction is well approximated by the functional form (1) used to parametrize the data, where the theory assumes a uniform free-carrier density throughout the system. The expected screening length is then $R_s=R_b$, which, for the samples described in Ref. 3 (free hole concentrations of $1.3-2.1\times10^{18}$ cm^{-3}), is between 3.0 and 3.8 nm. To obtain a surface screening length of 1.1 nm, as seen in the experiments, requires a hole concentration of 2×10^{19} cm^{-3}, an order of magnitude greater than the highest achievable free-carrier density in *p*-type InP.[13] This is inconsistent with the short local bulk screening length needed to explain the results of Ref. 3.

Independent experimental evidence suggests that it is inappropriate to assume a spatially uniform free-carrier density in the case of Ref. 3. Photoemission measurements indicate surface core level shifts of up to 0.5–0.6 eV following even very brief *in vacuo* anneals (200 °C) of freshly cleaved *p*-type InP(110) (free hole concentration 2×10^{18} cm^{-3}); the midgap pinning level is attributed to phosphorous surface vacancies.[14,15] Straightforward calculations show that much smaller surface potential shifts of $3-4k_BT$ ($\sim$0.1 eV) are sufficient to deplete the near-surface region of enough majority carriers that the surface screening length will increase tenfold over that inferred in Ref. 3. In short, depletion of the near-surface region means that bulk plasma properties are irrelevant to the interaction between surface charges in such a case.

One possible explanation for the unusually short screening length observed in Ref. 3 is free surface charge from a partially filled band of extrinsic surface states associated with the vacancies themselves. As noted in the Introduction, such free surface charge is not included in the present work.

VIII. SUMMARY

We have studied the electrostatic screening of point charges by an ideal semi-infinite semiconductor whose surface states do not contribute to the density of free carriers, applying Debye-Hückel theory to a system that is homogeneous in the bulk. This theory offers a quantitatively reliable picture of the electrostatic potential due to source charge above, within, and on the surface of a such a semiconductor, which is valid for length scales greater than a characteristic atomic dimension a. The theory also provides a number of important qualitative insights that contribute to our physical understanding of the more general coupled plasma-dielectric problem, including the following.

(1) If the source charge q is in *vacuum* and *far from* the surface (so that $z_0>0$ and $z_0\gg R_b$), then for an observer within a few R_b of the surface the metallic (plasma) properties of the semiconductor dominate. The electric field lines are orthogonal to the semiconductor surface, and the field is screened within R_b of the surface (Fig. 4). The surface charge distribution is extended radially, as for classical electrostatics.

(2) If the source charge q is in *vacuum* and *near* the surface (so that $z_0>0$ and $z_0\ll R_b$), then for an observer within a few z_0 of the surface the dielectric properties of the semiconductor dominate; the induced surface charge is as in the vacuum-dielectric case. Free and polarization charge within the semiconductor bulk causes screening for larger radial separations.

(3) If the source charge q is in the *semiconductor* and *near* the surface (so that $z_0<0$ and $|z_0|\ll R_b$), then for an observer within the bulk and near the surface, the semiconductor behaves like a dielectric. On going a few R_b further into the bulk, induced bulk charge (both free and polarization) completely screens q.

(4) If the source charge q is in the *semiconductor* and *far from* the surface (so that $z_0<0$ and $|z_0|\gg R_b$), the vacuum-semiconductor boundary plays no role; the system behaves like an infinite medium.

(5) If the source charge q describes a *semiconductor surface defect*, the electrostatic potential ϕ_s *along* the surface has two limiting behaviors. When ρ is small ($\rho<4R_b$), ϕ_s falls off exponentially, with characteristic length $R_b=R_b^{(0)}\sqrt{\varepsilon}$ and effective charge $2q/\varepsilon$. When ρ is large ($\rho>8R_b$), the source q is screened by induced surface charge, and together with induced bulk charge this generates a dipole potential that is zero on the surface, and a quadrupole potential that is nonzero. The dipole moment has strength $p=2qR_b/\varepsilon$, and the one independent quadrupole moment has strength $Q_{xx}=4qR_b^2/\varepsilon^2$.

The theory applies to ideal III-V(110) surfaces in the dilute defect limit, where it predicts a surface screening length equal to the bulk screening length. This is consistent with

well-established STM contour measurements.[2] The theory also provides a rigorous basis for the exponentially decaying interaction between two surface charges used to fit the pair correlation data in Ref. 3, but the screening length given by the theory is much longer than the experimentally observed one. Since the surface-charge density in these experiments is undoubtedly sufficient to cause free-carrier depletion, one might have expected the inequality to be reversed—that is, a surface screening length much longer than the bulk one. An additional source of screening charge is therefore needed to explain the results of Ref. 3. Because the intrinsic surface states associated with III-V(110) surfaces are insulating, they cannot provide this additional screening charge. Free charge in extrinsic surface states, on the other hand, may account for the unexpectedly short screening length. Generalization of the theory to include such free surface charge is presently underway.[16]

ACKNOWLEDGMENTS

This work was supported, in part, by grants from the Department of Energy and from the National Science Foundation, Division of Materials Research.

APPENDIX

1. Potentials for source above surface

Equation (4) is satisfied by the potential $\phi_v^{(1)}$ due to q localized at $\mathbf{r}_0$, which can be expanded in terms of the zeroth order Bessel function as[6]

$$\phi_v^{(1)}=\frac{q}{4\pi\varepsilon_0}\frac{1}{\sqrt{\rho^2+(z-z_0)^2}}=\frac{q}{4\pi\varepsilon_0}\int_0^\infty dk\,J_0(k\rho)\exp(-k|z-z_0|). \quad \text{(A1)}$$

However, the potential ϕ_v must be a sum of $\phi_v^{(1)}$ and an additional term $\phi_v^{(2)}$ that satisfies Laplace's equation, due to semiconductor in the region $z<0$. To expand $\phi_v^{(2)}$ in terms of $J_0(k\rho)$, we separate the variables ρ and z in $\phi_v^{(2)}$ as $\phi_v^{(2)}=\int_0^\infty dk\,C_v(k)R(k,\rho)Z(k,z)$. By well-known methods,[6] we obtain the equations for $R(k,\rho)$ and $Z(k,z)$. Their solutions are $R(k,\rho)=J_0(k\rho)$ and $Z(k,z)\sim\exp(-k|z|)$. Thus, $\phi_v^{(2)}$ must be expanded as

$$\phi_v^{(2)}=\frac{q}{4\pi\varepsilon_0}\int_0^\infty dk\,C_v(k)J_0(k\rho)\exp(-k|z|). \quad \text{(A2)}$$

From $\phi_v^{(1)}$ and $\phi_v^{(2)}$, by linear superposition, ϕ_v is

$$\phi_v=\frac{q}{4\pi\varepsilon_0}\int_0^\infty dk J_0(k\rho)[\exp(-k|z-z_0|)+C_v(k)\exp(-kz)] \quad (z>0). \quad \text{(A3)}$$

The solution of Eq. (7), for ϕ_b, is obtained similarly. We now write ϕ_b as

$$\phi_b=\int_0^\infty dk\,D_b(k)R(k,\rho)Z(k,z), \quad \text{(A4)}$$

where Z and R satisfy

$$\frac{d^2Z}{dz^2}-(k^2+k_b^2)Z=0 \quad \text{and} \quad \frac{d^2R}{d\rho^2}+\frac{1}{\rho}\frac{dR}{d\rho}+k^2R=0. \quad \text{(A5)}$$

Here $k_b=R_b^{-1}$, and R_b is defined in Eq. (2). Z must again be an exponentially decreasing function of z, so $Z(k,z)\sim\exp(-\sqrt{k^2+k_b^2}|z|$. The equation for R is again the differential equation for $J_0(k\rho)$.

From Eq. (A4), ϕ_b can be expanded as

$$\phi_b=\frac{q}{4\pi\varepsilon_0}\int_0^\infty dk\,D_b(k)J_0(k\rho)\exp(z\sqrt{k^2+k_b^2}) \quad (z<0). \quad \text{(A6)}$$

2. Potentials for source within semiconductor

If the source q is within the semiconductor, then $\nabla^2\phi_v=0$. Thus, from Eq. (A2),

$$\phi_v=\frac{q}{4\pi\varepsilon_0}\int_0^\infty dk\,C_v(k)J_0(k\rho)\exp(-kz) \quad (z>0). \quad \text{(A7)}$$

For $z<0$, the potential ϕ_b is obtained by linear superposition $\phi_b=\phi_b^{(1)}+\phi_b^{(2)}$, where $\phi_b^{(1)}$ satisfies Eq. (26), whereas $\phi_b^{(2)}$ satisfies Eq. (7). The solution to Eq. (7) has the same form as Eq. (9), so we can express $\phi_b^{(2)}$ as

$$\phi_b^{(2)}=\frac{q}{4\pi\varepsilon_0}\int_0^\infty dk\,D_b(k)J_0(k\rho)\exp(z\sqrt{k^2+k_b^2}) \quad (z<0). \quad \text{(A8)}$$

To obtain $\phi_b^{(1)}$ by solving Eq. (26), we expand the radial δ function in terms of the zeroth-order Bessel function, to obtain[6]

$$-\frac{1}{\varepsilon\varepsilon_0}\rho_b=-\frac{1}{\varepsilon\varepsilon_0}\frac{q}{2\pi}\int_0^\infty dk\,kJ_0(k\rho)\,\delta(z-z_0). \quad \text{(A9)}$$

We now expand $\phi_b^{(1)}$ as

$$\phi_b^{(1)}=\int_0^\infty dk\,kJ_0(k\rho)Z(z,z_0;k) \quad (z<0). \quad \text{(A10)}$$

From Eqs. (26) and (A10), the function Z must satisfy

$$\frac{d^2Z}{dz^2}-(k^2+k_b^2)Z=-\frac{1}{\varepsilon\varepsilon_0}\frac{q}{2\pi}\delta(z-z_0). \quad \text{(A11)}$$

Using methods in Ref. 6, we find that

$$Z(z,z_0;k)=\frac{q}{4\pi\varepsilon_0}\frac{1}{\varepsilon\sqrt{k^2+k_b^2}}\exp(-\sqrt{k^2+k_b^2}|z-z_0|). \quad \text{(A12)}$$

Thus, combining Eqs. (A8), (A10), and (A12), we find that

$$\phi_b=\frac{q}{4\pi\varepsilon_0}\int_0^\infty dk\,J_0(k\rho)\left(\frac{k}{\varepsilon\sqrt{k^2+k_b^2}}\exp(-\sqrt{k^2+k_b^2}|z-z_0|)+D_b(k)\exp(z\sqrt{k^2+k_b^2})\right). \quad \text{(A13)}$$

3. Surface potential at large radial distances

To obtain the large ρ limiting behavior, we substitute $k\rho = x$ in Eq. (34). Then

$$\phi_s = \frac{q}{4\pi\varepsilon_0}\frac{2}{\rho}\int_0^\infty dx\, J_0(x)\frac{x}{x+\varepsilon\sqrt{x^2+(k_b\rho)^2}}. \quad \text{(A14)}$$

To the ratio term of the integrand in Eq. (A14), we add and subtract its limit as $x\to\infty$, $1/(\varepsilon+1)$. This gives

$$\phi_s = \frac{q}{4\pi\varepsilon_0}\frac{2}{\varepsilon+1}\frac{1}{\rho}\int_0^\infty dx\, J_0(x) + \frac{q}{4\pi\varepsilon_0}\frac{2\varepsilon}{\varepsilon+1}\frac{1}{\rho}\int_0^\infty dx\, J_0(x)\frac{x-\sqrt{x^2+(k_b\rho)^2}}{x+\varepsilon\sqrt{x^2+(k_b\rho)^2}}. \quad \text{(A15)}$$

The first term in Eq. (A15) is integrable analytically, yielding

$$\phi_s = \frac{q}{4\pi\varepsilon_0}\frac{2}{\varepsilon+1}\frac{1}{\rho}\times\left[1+\varepsilon\int_0^\infty dx\, J_0(x)\frac{x-(k_b\rho)\left[1+\left(\frac{x}{k_b\rho}\right)^2\right]^{1/2}}{x+\varepsilon(k_b\rho)\left[1+\left(\frac{x}{k_b\rho}\right)^2\right]^{1/2}}\right]. \quad \text{(A16)}$$

We now divide the numerator and the denominator of the integrand of the second term in Eq. (A16) by $k_b\rho$, and then expand both up to the second order in $x/k_b\rho$. Also, to enable further expansion, we multiply the integrand by $\exp(-\delta x)$, and take the limit $\delta\to 0$. This gives

$$\phi_s = \frac{q}{4\pi\varepsilon_0}\frac{2}{\varepsilon+1}\frac{1}{\rho}\left(1-\lim_{\delta\to 0}\int_0^\infty dx\, J_0(x)\times\exp(-\delta x)\frac{1-\frac{x}{k_b\rho}+\frac{1}{2}\left(\frac{x}{k_b\rho}\right)^2}{1+\frac{1}{\varepsilon}\frac{x}{k_b\rho}+\frac{1}{2}\left(\frac{x}{k_b\rho}\right)^2}\right). \quad \text{(A17)}$$

Further expansion in Eq. (A17) gives

$$\phi_s = \frac{q}{4\pi\varepsilon_0}\frac{2}{\varepsilon+1}\frac{1}{\rho}\left[1-\lim_{\delta\to 0}\int_0^\infty dx\, J_0(x)\exp(-\delta x)\times\left(1+\frac{1}{\varepsilon}x+\frac{\varepsilon+1}{\varepsilon^2}\frac{1}{(k_b\rho)^2}x^2\right)\right]. \quad \text{(A18)}$$

In Eq. (A18), the first integral cancels the 1, the second integral is zero, and the third integral gives Eq. (36).

4. Total surface charge for $z_0k_b \ll 1$ and $z_0k_b \gg 1$

We now determine, analytically, the total surface charge q_s from the surface charge density σ_s in the limits $z_0k_b \ll 1$ and $z_0k_b \gg 1$. Our result, derived for $z>0$, is also valid for $z_0<0$.

From Eqs. (15) and (16), the total surface charge q_s is given by

$$q_s = -q(\varepsilon-1)\int_0^\infty d\rho\,\rho\int_0^\infty dk\, J_0(k\rho)\frac{k\sqrt{k^2+k_b^2}}{k+\varepsilon\sqrt{k^2+k_b^2}}\times\exp(-kz_0). \quad \text{(A19)}$$

In order to reverse the order of integration in Eq. (A19), we multiply the integrand by $\exp(-\delta\rho)$, and take the limit $\delta\to 0$. Further, changing the variables to $x=kz_0$ and $\delta' = z_0\delta$, we obtain

$$q_s = -q(\varepsilon-1)\lim_{\delta'\to 0}\delta'\times\int_0^\infty dx\frac{x\sqrt{x^2+(k_bz_0)^2}}{x+\varepsilon\sqrt{x^2+(k_bz_0)^2}}\frac{\exp(-x)}{\sqrt{x^2+\delta'^2}^3}. \quad \text{(A20)}$$

For $z_0k_b \ll 1$, we neglect terms z_0k_b in the integrand (which remains finite even for $x=0$), and obtain

$$q_s = -q(\varepsilon-1)\lim_{\delta'\to 0}\delta'\int_0^\infty dx\frac{x}{\varepsilon+1}\frac{\exp(-x)}{\sqrt{x^2+\delta'^2}^3}. \quad \text{(A21)}$$

Finally, we set $x=y\delta'$ in Eq. (A21) to obtain

$$q_s = -q\frac{\varepsilon-1}{\varepsilon+1}\lim_{\delta'\to 0}\int_0^\infty dy\frac{y}{\sqrt{y^2+1}^3}\exp(-y\delta') = -q\frac{\varepsilon-1}{\varepsilon+1} \quad (z_0k_b \ll 1). \quad \text{(A22)}$$

If $z_0k_b \gg 1$, then z_0k_b is much larger than any x value that contributes significantly to Eq. (A20), since the integrand falls off as $\exp(-x)$. Thus, we can neglect x in the term $\sqrt{x^2+(z_0k_b)^2}$ of Eq. (A20), which gives

$$q_s = -q(\varepsilon-1)\lim_{\delta'\to 0}\int_0^\infty dx\frac{xk_bz_0}{x+\varepsilon k_bz_0}\frac{\exp(-x)}{\sqrt{x^2+\delta'^2}^3}. \quad \text{(A23)}$$

In the first term of the integrand, we neglect x in the denominator. This gives an integrand proportional to that in Eq. (A21), resulting in

$$q_s = -q(\varepsilon-1)\lim_{\delta'\to 0}\delta'\int_0^\infty dx\frac{x}{\varepsilon}\frac{\exp(-x)}{\sqrt{x^2+\delta'^2}^3} = -q\frac{\varepsilon-1}{\varepsilon} \quad (k_bz_0 \gg 1). \quad \text{(A24)}$$

[1] See, for example, C.B. Duke, J. Vac. Sci. Technol. A **10**, 2032 (1992); or J.P. LaFemina, Surf. Sci. Rep. **16**, 133 (1992), and references therein.
[2] J.A. Stroscio and R.M. Feenstra, in *Methods of Experimental Physics*, edited by J.A. Stroscio and W.J. Kaiser (Academic, Press, New York, 1993), Vol. 27.
[3] P. Ebert, X. Chen, M. Heinrich, M. Simon, K. Urban, and M.G. Lagally, Phys. Rev. Lett. **76**, 2089 (1996).
[4] Neil W. Ashcroft and N. David Mermin, *Solid State Physics* (Holt, Rinehart and Winston, New York, 1975).
[5] R.B. Dingle, Philos. Mag. **46**, 831 (1955).
[6] J.D. Jackson, *Classical Electrodynamics*, 2nd ed. (Wiley, New York, 1975).
[7] Z.-H. Zhang, M. Weimer, and R.E. Allen, Phys. Rev. B **48**, 15 068 (1993).
[8] I.S. Gradshteyn and I.M. Ryzhik, *Table of Integrals, Series and Products* (Academic Press, New York, 1965).
[9] B. Roulet and M. St. Jean, Am. J. Phys. (to be published).
[10] William H. Press, Saul A. Teukolsky, William T. Vetterling, and Brian P. Flannery, *Numerical Recipes* (Cambridge University Press, New York, 1992).
[11] M. Medina-Noyala and B. Ivlev, Phys. Rev. E **52**, 6281 (1995).
[12] Kim A. Sharp and Barry Honig, J. Phys. Chem. **94**, 7684 (1990).
[13] E.F. Schubert, *Doping in III-V Semiconductors* (Cambridge University Press, New York, 1993).
[14] M. Yamada, A.K. Wahi, P.L. Meissner, A. Herrera-Gomez, T. Kendelewicz, and W.E. Spicer, Appl. Phys. Lett. **58**, 2243 (1991).
[15] M. Yamada, A.K. Wahi, T. Kendelewicz, and W.E. Spicer, Phys. Rev. B **45**, 3600 (1992).
[16] M. Krcmar, W.M. Saslow, and M.B. Weimer (unpublished).